Ceramics International 42 (2016) 11640–11649

Contents lists available at ScienceDirect

Ceramics International

journal homepage: www.elsevier.com/locate/ceramint

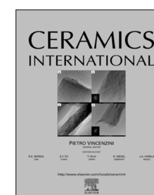

Microstructure, optical and electrical properties of sputtered HfTiO high-k gate dielectric thin films

S.S. Jiang [a], G. He [a,d,*], J. Gao [a,b], D.Q. Xiao [a], P. Jin [a], W.D. Li [a], J.G. Lv [c,**], M. Liu [d,**], Y.M. Liu [a], Z.Q. Sun [a]

[a] School of Physics and Materials Science, Radiation Detection Materials & Devices Lab, Anhui University, Hefei 230601, PR China
[b] School of Sciences, Anhui University of Science and Technology, Huainan 232001, PR China
[c] Department of Physics and Electronic Engineering, Hefei Normal University, Hefei 230061, PR China
[d] Key Laboratory of Materials Physics, Anhui Key Laboratory of Nanomaterials and Nanostructure, Institute of Solid State Physics, Chinese Academy of Sciences, Hefei 230031, PR China

ARTICLE INFO

Article history:
Received 26 March 2016
Received in revised form
13 April 2016
Accepted 13 April 2016
Available online 14 April 2016

Keywords:
C. Electrical properties
High-k gate dielectrics
Metal–oxide–semiconductor
Conduction mechanisms
Sputtering

ABSTRACT

The microstructure, optical and electrical properties of HfTiO high-k gate dielectric thin films deposited on Si substrate and quartz substrate by RF magnetron sputtering have been investigated. Based on analysis from x-ray diffraction (XRD) measurements, it has been found that the as-deposited HfTiO films remain amorphous regardless of the working gas pressure. Meanwhile, combined with characterization of ultraviolet-visible spectroscopy (UV–vis) and spectroscopy ellipsometry (SE), the deposition rate, band gap and optical properties of sputtered HfTiO gate dielectrics were determined. Besides, by means of the characteristic curves of high frequency capacitance–voltage (*C–V*) and leakage current density–voltage (*J–V*), the electrical parameters, such as permittivity, total positive charge density, border trap charge density, and leakage current density, have been obtained. The leakage current mechanisms are also discussed. The energy band gap of 3.70 eV, leakage current density of 1.39×10^{-5} A/cm^2 at bias voltage of 2 V, and total positive charge density and border trap charge density of 9.16×10^{11} cm^{-2} and 1.3×10^{11} cm^{-2}, respectively render HfTiO thin films deposited at 0.6 Pa, potential high-k gate dielectrics in future CMOS devices.

© 2016 Elsevier Ltd and Techna Group S.r.l. All rights reserved.

1. Introduction

With the rapid development of ultra large scale integrated circuit (ULSIC), the conventional SiO_2-based high-k gate dielectrics in CMOS devices have been outdated because its thickness cannot reach the limit below 1.0 nm [1]. Therefore, many high dielectric constant (*k*) materials such as Hf-based and Zr-based gate dielectrics are attracting an increasing interest as a solution for the saturation of the leakage current and the power consumption of SiO_2 CMOS [2–5]. Among these high-k candidates, HfO_2 has been investigated as an alternative gate dielectric material to conventional SiO_2 due to its moderate dielectric constant (~25), wide band gap (~5.8 eV), superior thermodynamic stability and appropriate band offset relative to Si substrate [6,7]. However, pure HfO_2 has low crystallization temperature, resulting in large leakage current, high oxygen and impurities penetration, and defect generation [8]. One of the effective ways to increase the crystallization temperature and decrease the charge leakage is combining it with another complementary gate materials, such as TiO_2. Recent investigations have indicated that Ti is one of the most suitable elements incorporated into HfO_2 due to the superior k value (80–100) of TiO_2 [9,10]. Besides, it can be noted that Hf and Ti are both 4-valence elements which would restrain the production of oxygen vacancy dramatically, thereby reducing the leakage current density [11]. Furthermore, TiO_2 have high crystallization temperature. Ye et al. have showed that the amorphous TiO_2 crystallizes at 873 K and 1073 K to form TiO_2 with the anatase phase and the rutile phase TiO_2, respectively [12].

Currently, considerable works has been devoted to control the deposition power, annealing temperature, substrate temperature and concentration of Ti to obtain HfTiO gate dielectric thin films with high quality [13]. Liu et al. have reported that Ti incorporated into HfO_2 would strengthen its interfacial properties and reduce the thickness of interfacial layer. In addition, the band gap

* Corresponding author at: School of Physics and Materials Science, Radiation Detection Materials & Devices Lab, Anhui University, Hefei 230601, PR China.
** Corresponding authors.
E-mail addresses: hegang@ahu.edu.cn (G. He), jglv@hftc.edu.cn (J.G. Lv), mliu@issp.ac.cn (M. Liu).

http://dx.doi.org/10.1016/j.ceramint.2016.04.067
0272-8842/© 2016 Elsevier Ltd and Techna Group S.r.l. All rights reserved.

decreases with the increase of Ti concentration [14]. Besides, it has been shown by Ye that rapid thermal annealing at 600 °C can obtain the largest dielectric constant of 45.9, the lowest leakage current of 3.1×10^{-6} A/cm^2, and the optimized interfacial properties [12]. However, there is little works which focus on the investigation of the working gas pressure dependent microstructure, optical and electrical properties of HfTiO/SiO_2/Si gate stacks. In fact, it is worth investigating systematically since that the working gas pressure is expected to be a key factor which influences the deposition rate, energy band gap, optical constants and electrical properties of as-deposited thin films.

In current work, the microstructure, optical and electrical properties of HfTiO gate dielectrics subjected to different working gas pressure were investigated systematically by means of characterization from x-ray diffraction (XRD), energy dispersive X-ray spectroscopy (EDS), ultraviolet–visible spectroscopy (UV–vis), spectroscopy ellipsometry (SE), high frequency capacitance–voltage (*C*–*V*) and current density–voltage (*J*–*V*) measurements.

2. Experimental procedure

2.1. Preparation of films

Commercially available n-type (100) Si wafers with a resistivity of 2–5 Ω/cm were chosen as the substrates. To obtain the optical properties preferably, the quartz plates were also chosen as the substrates. Prior to HfTiO thin films deposition, the substrates were ultrasonically cleaned by ethanol for 10 min at room temperature, washed with a standard Radio Corporation of American (RCA) for 10 min at 75 °C to remove organic and metallic impurities on the wafers, and immersed in a diluted HF solution for 20 s to remove any native oxide and dried by high purity nitrogen. After cleaning, the Si and quartz substrates were loaded into the vacuum chamber of a magnetron sputtering equipment (JGP-DZS, Chinese Academy of Sciences, Shenyang Scientific Instrument Co., Ltd.) immediately. Before deposition, the vacuum chamber was evacuated to 5.0×10^{-4} Pa. The radio frequency reactive sputtering of HfTi alloy target was employed to deposit HfTiO thin films on the Si and quartz substrates in Ar and O_2 ambient with the flow rates of 20 and 2 SCCM (SCCM denotes cubic centimeter per minute at STP), respectively. The RF power, deposition time, and deposition temperature were fixed at 50 W, 1 h, and room temperature, respectively. The working gas pressure of Ar varied from 0.2 to 0.8 Pa at a pressure interval of 0.2 Pa. Besides, the target was pre-sputtered in an argon atmosphere for 10 min before the film deposition to remove the native oxide.

2.2. Film characterization

The microstructure of the as-deposited films were investigated by X-ray diffraction (XRD, MXP 18AHF MAC Science, Yokohama, Japan). The X-ray source was $CuK\alpha$, with an accelerating voltage of 40 KV, a current of 100 mA, scanning range from 20 °C to 80 °C, glancing angle of 2 °C, scanning step of 0.02 °C, and scanning speed of 8 °C/min. And the component and weight percentage of HfTiO thin films were obtained by energy dispersive X-ray spectroscopy (EDS). In addition, the spectroscopy ellipsometry (SC630, SANCO Co., Shanghai) in the spectrum range of 900–1100 nm with a step of 10 nm at an incident angle of 65 °C and 75 °C was used to determine the thickness, refractive index, extinction coefficient and dielectric dispersion of the as-deposited samples. In the process of fitting, the optical constants can be obtained from the Cauchy–Urbach dispersion model which consists of three layer structure: thickness-fixed Si substrate, SiO_2 interfacial layer, and HfTiO gate dielectric. And the transmission spectrum and absorption spectrum were investigated by ultraviolet–visible spectroscopy (UV–vis, Shirmadzu,UV-2550). The energy band gap values of the films can be obtained from absorption spectrum via optical method.

2.3. Metal oxide semiconductor (MOS) device fabrication and characterization

In order to explore the electrical properties, a series of MOS capacitors were fabricated by sputtering a Al-top electrode with the area of 7.065×10^{-8} m^2 through a shadow mask and Al was also deposited as the back electrode to decrease the contact resistance. The high-frequency (1 MHZ) *C*–*V* curves and leakage current characteristics were performed using an semiconductor device analyzer (Agilent B1500A) and Cascade Probe Station. All the electrical tests were required to short circuit and open circuit calibration, and carried out at room temperature in a dark box.

3. Results and discussion

3.1. Crystal structure and component analysis

In order to investigate the effect of working pressure on the microstructure of sputtering-grown HfTiO samples, XRD spectra has been examined, as presented in Fig. 1. It can be noted that all samples remain amorphous state with the increase of the working pressure. It has been reported that high-k gate dielectrics with amorphous structure will be preferable for CMOS devices application, since the grain clearance of polycrystalline materials would provide a current channel, thus resulting in large leakage current and low reliability of the devices [11,15]. Besides, based on previous investigation, it can be noted that the as-deposited HfO_2 film has one major diffraction peak located at $2\theta=28.35°$ and some smaller peaks at other positions [16], indicating that the crystallization temperature of HfO_2 films has been improved remarkably after TiO_2 incorporation. One major reason for the formation of amorphous structure is the fact that TiO_2-doped HfO_2 film produce more nucleation sites and thereby prevents the growth of crystal grains by turns [17]. Another reason is that Hf and Ti have different ionic radii which inhabits the formation of long-range order structure [8].

Fig. 2 illustrates the working gas pressure dependent EDS spectra of the as-deposited HfTiO films. It has been found that all

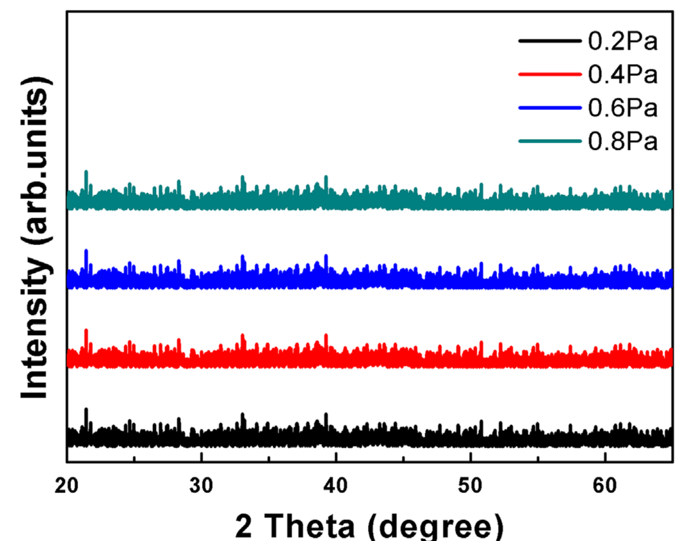

Fig. 1. XRD patterns of HfTiO thin films deposited at various working pressure.

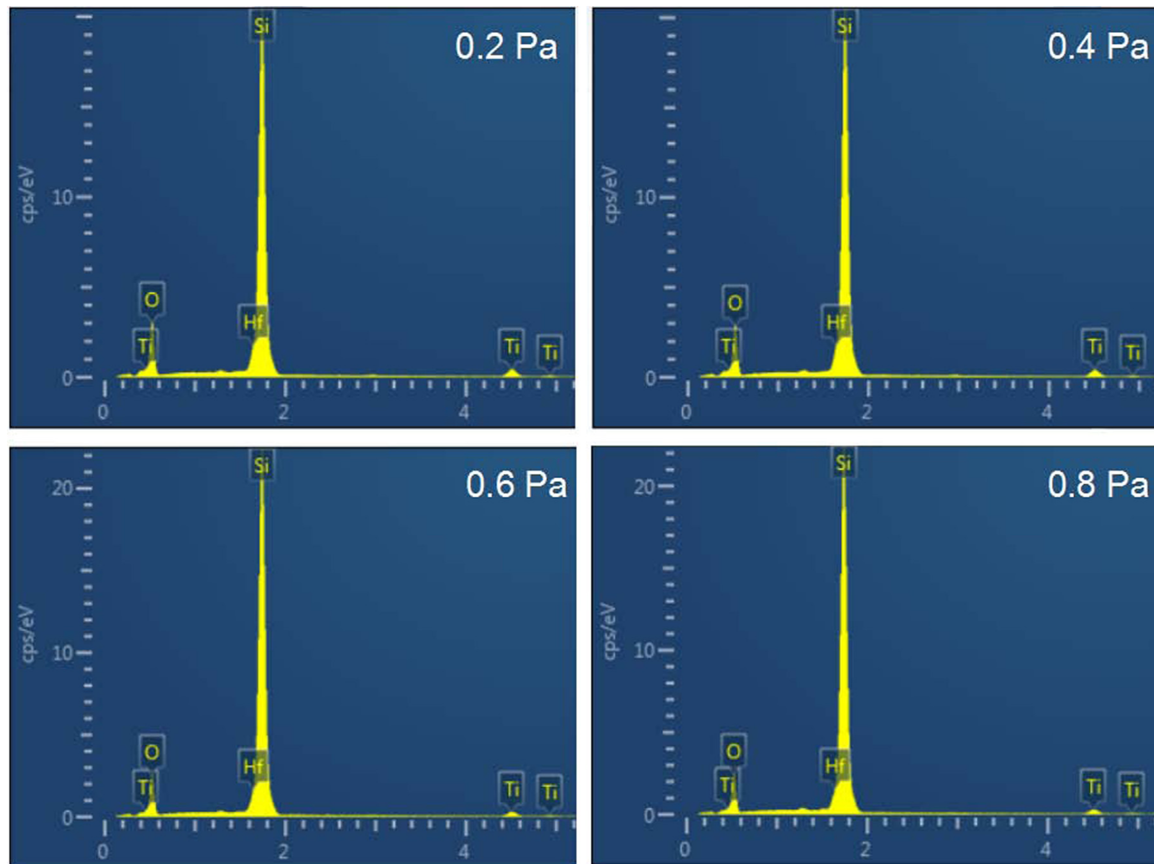

Fig. 2. The EDS spectra of HfTiO/Si gate stacks with different working pressure.

Table 1
Weight percentage of the components of HfTiO thin film at various working pressure.

Working pressure (Pa)	Hf (wt%)	Ti (wt%)	Hf:Ti
0.2	12.12	8.98	1:2.7
0.4	12.35	8.35	1:2.5
0.6	10.45	6.39	1:2.2
0.8	10.46	6.33	1:2.2

samples consist of Hf, Ti, O and the Si element which results from the Si substrate. The specific weight percentages of the films are demonstrated in Table 1. It is calculated that the atomic percentage of Hf and Ti is close to that of the sputtering target.

3.2. Optical properties investigation

UV–vis spectroscopy was used to obtain the transmittance spectrum and the absorption spectrum of HfTiO thin films deposited on quartz glass substrates at room temperature within 260–900 nm wavelength range. Fig. 3 exhibits the transmittance spectrum of thin films with the working pressure ranging from 0.2 to 0.4 Pa. From Fig. 3, it can be noted that the transmittance of the thin film samples in the visible light region is more than 75%, which can be attributed to the uniform microstructure [18]. Furthermore, the absorption edges present a slightly red shift from 0.2 to 0.4 Pa and an apparent blue shift from 0.4 to 0.8 Pa.

It is generally known that the insulator optical absorption law is closely related to energy gap structure. And the absorption coefficient α is also combined with the energy band gap E_g in the form of

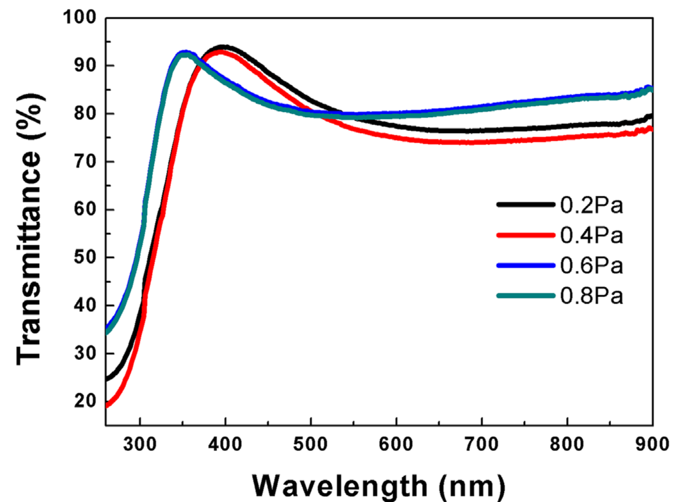

Fig. 3. Transmission spectra for sputtering-derived HfTiO thin films deposited at various working pressure.

$$(\alpha h\nu)^{1/2} = A\left(h\nu - E_g\right) \quad (1)$$

In which A is a constant characteristic of the semiconductor, $h\nu$ is the photon energy. Plot of $(\alpha h\nu)^{1/2}$ vs $(h\nu)$ was shown in Fig. 4 and the optical band gap energy E_g can be obtained by extrapolating the linear portion of the curves relating $(\alpha h\nu)^{1/2}$ and $(h\nu)$ to $(\alpha h\nu)^{1/2} = 0$. The extracted band gap values of 3.59, 3.52, 3.70 and 3.77 eV have been determined as the working gas pressure changes from 0.2 Pa to 0.8 Pa. It can be seen clearly that the optical band gap is in the range of 3.59–3.77 eV and gradually shifts to low energy side and then rapidly increases as the pressure increases.

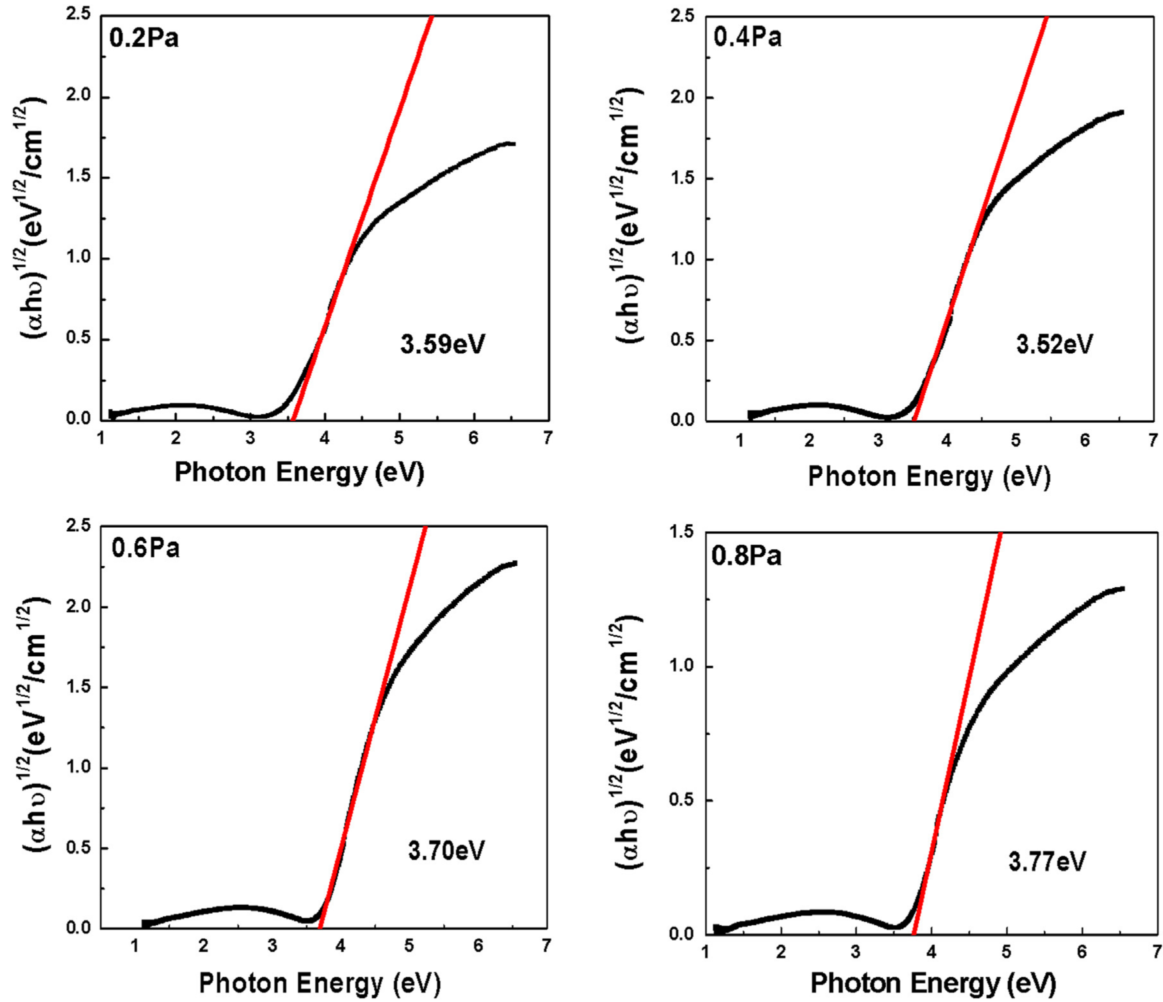

Fig. 4. Plots of $(\alpha h\nu)^{1/2}$ versus the photon energy $h\nu$ for HfTiO thin films grown on quartz substrate.

This transformation of band gap of HfTiO thin films agree with well the result of transmission spectra, as shown in Fig. 3. It is believed that the packing density and oxygen content of HfTiO thin films may be the key factors to result in this dramatic conversion. And the energy band gap decreases with the increases of packing density and the decreases of oxygen content [19–21].

Spectroscopic ellipsometry (SE) is a fast and sensitive method to characterize the optical properties of thin films. During measurements, it requires no special environment and touching samples are not needed. In current work, the SE was adopted to obtain working gas pressure dependent optical functions of HfTiO thin films in the spectral range of 300–1100 nm, step of 10 nm, at 65° and 70° angles of incidence. The spectral dependence of experimental parameters ψ (azimuth) and Δ (phase change) are related to the structural and optical properties of thin films given by

$$\rho = \frac{R_p}{R_s} = \tan\psi \exp(i\Delta) \tag{2}$$

In which R_p and Rs are the amplitude reflection coefficient for the light polarized parallel (p) and perpendicular (s) to the plane of incidence, respectively. When appropriate model have been selected, the thickness and optical properties of the films can be simultaneously obtained by the fitting results. Through a series of comparative analysis, Cauchy-Urbach model has been adopted to characterize the dielectric function of HfTiO thin films expressed as following formula

$$n(\lambda) = A_n + \frac{B_n}{\lambda^2} + \frac{C_n}{\lambda^4} \tag{3}$$

$$k(\lambda) = \alpha \exp\left(\beta\left(\frac{1240}{\lambda} - E_g\right)\right) \tag{4}$$

Formulae (3) and (4) as a function of the wavelength λ are uniquely defined by six parameters: A_n, B_n, C_n (index parameters which specify the index of refraction), α (ectinction coefficient amplitude), β (exponent factor), and E_g (band edge). In current work, a three-phase optical model consisting of the Si substrate, the interfacial layer and the HfTiO thin film was used to reach a good consistency between the measured and the theoretical data. Fig. 5 shows the measured and fitted spectra of a representative HfTiO thin film at a working pressure of 0.6 Pa. It can be seen from Fig. 5 that the experimental data are in good agreement with the fitted data for HfTiO thin film in the fully measured energy range, suggesting that the three-phase structured model is practicable and the thickness and optical properties of HfTiO thin films can be confirmed precisely.

The thicknesses of the thin films obtained based on the fitting results are 19.52, 13.00, 15.65 and 19.89 nm for 0.2, 0.4, 0.6, and 0.8 Pa, respectively. Fig. 6 presents the deposition rate as a function of the working gas pressure. From Fig. 6, it can be seen that the deposition rate increases when the Ar flow rate increases, which can be attributed to the fact that during working pressure from 0.2 Pa to 0.4 Pa, the quantity of incident ion and ion current

(I) increases. Meanwhile, the deposition rate Q is related to the ion current I in the form of

$$Q = CIS \quad (5)$$

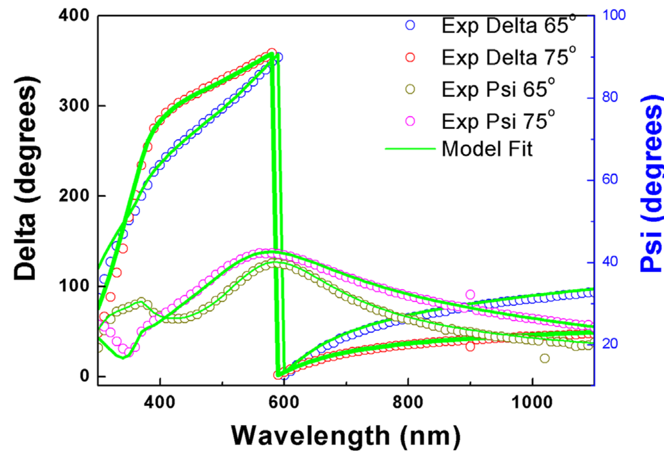

Fig. 5. Measured and fitted ellipsometric parameters Δ and ψ for HfTiO thin films with working pressure of 0.6 Pa at the incident angle of 65 °C and 75 °C.

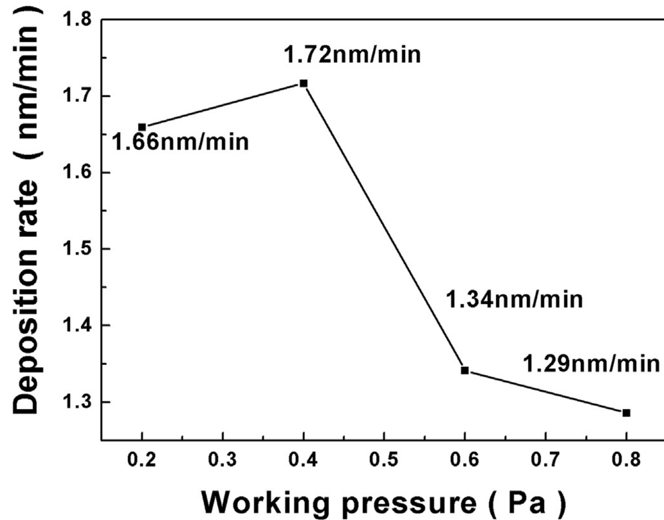

Fig. 6. The deposition rate of HfTiO thin films with the working pressure.

In which C is the characteristic constant related to the sputtering equipment and S is the sputtering rate, respectively [22]. It is this direct ratio relationship that result the deposition rate increase. However, the Q values decrease from 1.72 through 1.34–1.29 as the working pressure changes from 0.4 Pa through 0.6–0.8 Pa, respectively. According to kinetic theory of gases, the mean free path of gas molecules $\bar{\lambda}$ and the pressure P has the following relationship

$$\bar{\lambda} = \frac{KT}{\sqrt{2}\pi d^2 P} \quad (6)$$

In which K is the boltzmann constant, T is the gas temperature, d is the diameter of gas molecules, respectively. Based on the Eq. (6), the reduction in free path has been detected with increasing the working pressure on condition that the molecular diameter and gas temperature remain unchanged, which brings about the enhancement of collision frequency between the sputtered atoms and Ar gas molecules. Therefore, the energy of sputtered atom would lost greatly in the process of collision and then result in the decreases in particles number arrived at Silicon substrate [23]. Consequently, the deposition rate decreases.

Fig. 7 exhibits the variation of the refractive index n and the real part of dielectric function ε_1 of the HfTiO thin films dependence of wavelength at different working pressure. It can be found that the refractive index of thin film increases a little when the working gas pressure increases from 0.2 Pa to 0.4 Pa, and decreases rapidly with a further increase of working pressure. This phenomenon may be ascribed to the fact that the sputtering particles with high energy will result in high packing density and thus high refractive index [24]. As is well known, the packing density is a critical factor to affect the refractive index. In addition, the packing density may be correlated to the thickness of thin film [25]. The deposition rate can be obtained by the thickness of thin film divided by same deposition time. If the thin film is deposited at a higher rate, the higher particle energy can be obtained and thus higher mobility prompts the particles to form more denser HfTiO thin films. At a lower deposition rate, the thin film with lower refractive index will be obtained with a loose arrangement. The real part of the dielectric function ($\varepsilon_1 = n^2 - k^2$) be approximately equal to n^2 and is related to polarization. The intensity of polarization decreases with the refractive index increases and further lead to the increase of dielectric constant [25].

The effect of the working pressure on the extinction coefficient k and the imaginary part of dielectric function ($\varepsilon_2 = 2nk$) has also

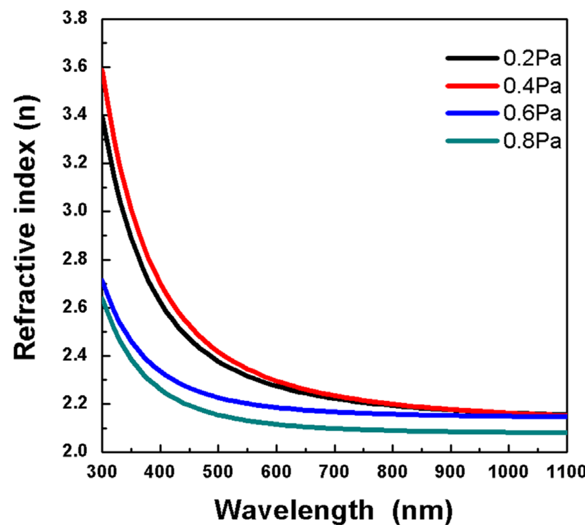

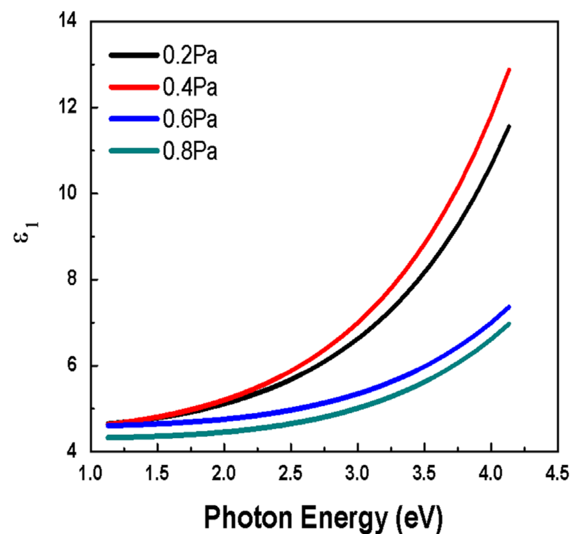

Fig. 7. The variation of optical refractive index n and real part of the dielectric functions extracted from the fitting of Cauchy model with the working pressure.

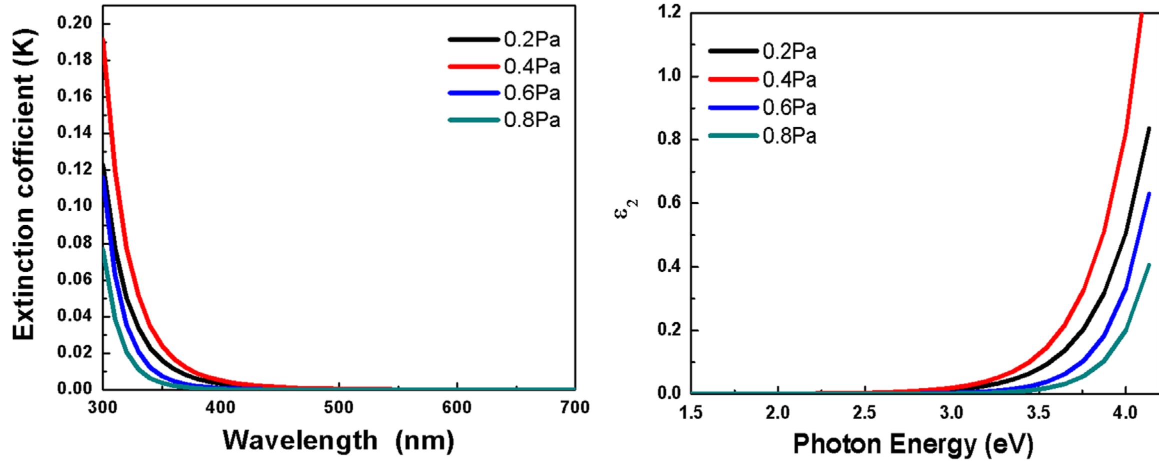

Fig. 8. The extinction coeffcient and imaginary parts of the dielectric functions of HfTiO thin films with various working pressure.

been studied, as shown in Fig. 8. It is easily found that the extinction coefficient and imaginary part of dielectric function of HfTiO thin films are close to zero in the high energy region and very low in the visible and near ultraviolet region. Besides, the red shift and the blue shift as a function of working pressure has been detected, which are confirmed by UV–vis measurement.

The absorption coefficient α can be calculated by the following expression:

$$\alpha = \frac{4\pi k}{\lambda} \tag{7}$$

where α is the absorption coefficient, λ is the light wavelength, and k is the extinction coefficient. Based on the relationship between extinction coefficient k and absorption coefficients (α), α versus hv plots of the as-deposited films have been shown in Fig. 9. So, the optical band gap can be extracted by extrapolating $[\alpha(E)]^{1/2}$ to zero, as shown in Fig. 10, which agree with the conclusion confirmed by UV–vis spectroscopy.

3.3. Electrical properties analysis

The typical *C–V* characteristics of MOS capacitors based on HfTiO high-k gate dielectrics as a function of working gas pressure

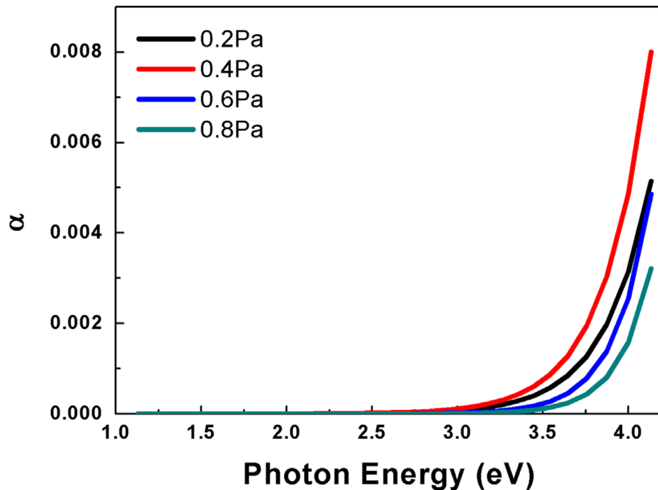

Fig. 9. The absorption coefficient α obtained from the the extinction coeffcient for HfTiO thin films with various working pressure.

measured at 1 MHz has been depicted in Fig. 11. Seen from the Fig. 11, the characteristic curves consist of the accumulation, the depletion, and inversion region, which are greatly similar to normal *C–V* curve and the film deposited at 0.6 Pa has the highest accumulation capacitance C_{ox} of 740 pF. According to the accumulation capacitance (C_{ox}), the equivalent oxide thickness (E_{ot}) and the dielectric constant (K_{hk}) can be extracted as shown in Table 2, which is expressed as follow

$$E_{ot} = \frac{K_{sio_2} \times \varepsilon_0}{C_{ox}/A} \tag{8}$$

$$K_{hk} = \frac{K_{sio_2} \times t_{hk}}{E_{ot} - t_{sio_2}} \tag{9}$$

In which K_{sio_2} is the dielectric constant of bulk sio_2 with the determined value of 3.9, ε_0 is the permittivity of vacuum, A is area of Al electrodes, the t_{hk} and t_{sio_2} is the physical thickness of HfTiO thin film and sio_2 interfacial layer, respectively [26]. It can be seen that the working pressure at 0.6 Pa has the smallest equivalent oxide thickness of 3.30 nm and the highest permittivity of 39.92.

The value of flat band voltage V_{fb} and hysteresis ΔV_{fb} can be obtained through the C_{fb} values from *C–V* curve respectively. The flat band capacitance C_{fb} was calculated by the expression

$$C_{fb} = \frac{C_{ox}}{1 + \frac{\varepsilon_{hk}}{\varepsilon_{rs} d_{ox}} \sqrt{\frac{kT\varepsilon_0\varepsilon_{rs}}{q^2 N_A}}} \tag{10}$$

In which ε_{hk} is the dielectric constant of HfTiO thin film, ε_{rs} is the dielectric constant of silicon wafer with the value of 11.9, N_A is the doping concentration of substrate, respectively [26]. The V_{fb} is closely related to the deficiencies in thin film and interface traps at interface layer and the negative V_{fb} indicates there much positive oxide charges while less negative oxide changes in the films [3,9]. Apparently, it can see from Table 2 the sample with the working pressure of 0.4 Pa has the highest absolute V_{fb} of 0.16 V, suggesting that this sample contains more defects and traps than the other samples. Table 2 also shows the density of the total positive charges (N_{total}) given by: $N_{total} = C_{ox}(\varphi_{ms} - V_{fb})/Aq$, in which the φ_{ms} is the work function between Al electrode and Si substrate (0.06 eV) [27]. According to Table 2, the N_{total} of the thin film at 0.4 Pa are 1.48×10^{12} cm^{-2}, others are smaller than 10^{11} cm^{-2}, which indicates that the thin films deposited at 0.2, 0.6 and 0.8 Pa are more favorable for the high dielectric films in the MOS application. Besides, the border trapped oxide charge density can be calculated through the anticlockwise hysteresis ΔV_{fb} by using the

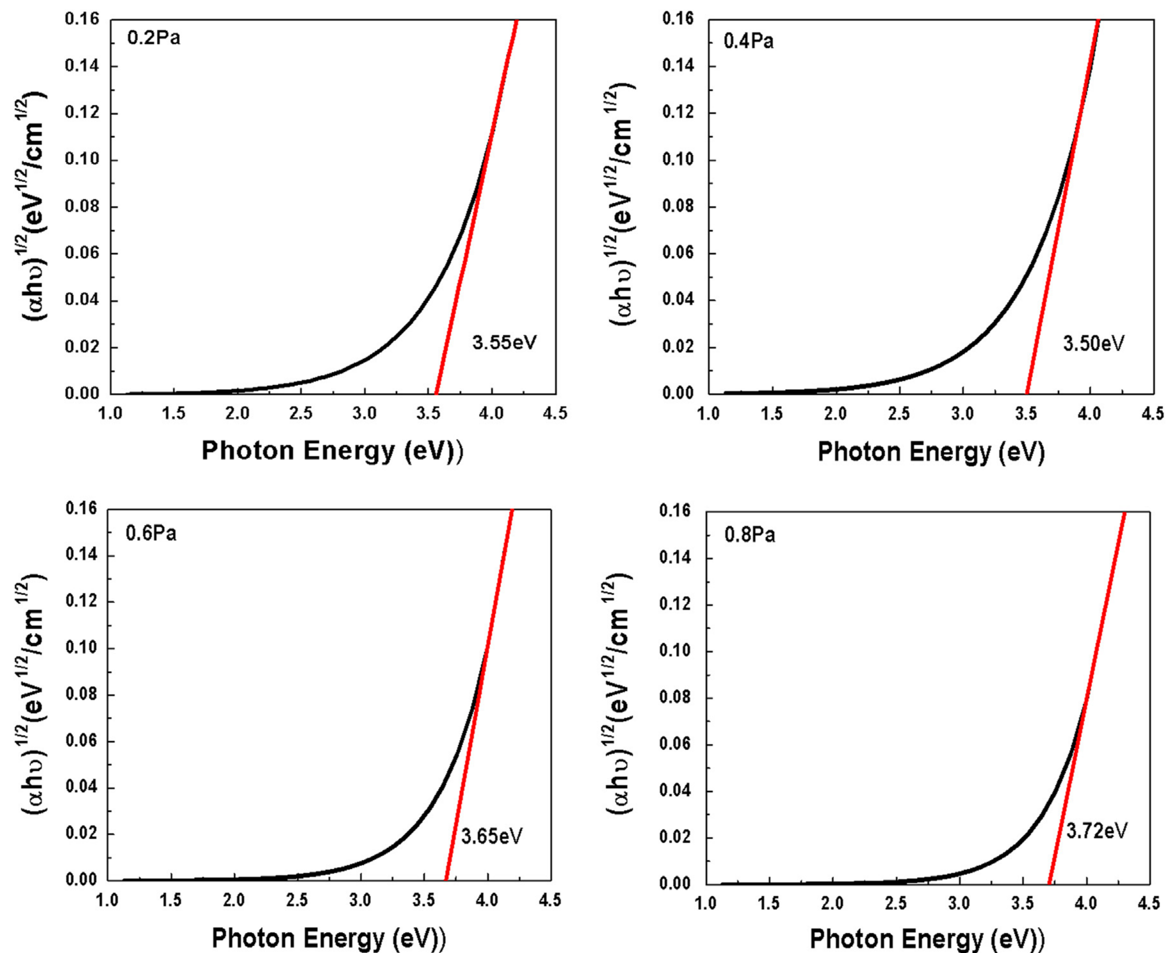

Fig. 10. The energy band gap obtained from the SE model fitting with different working pressure.

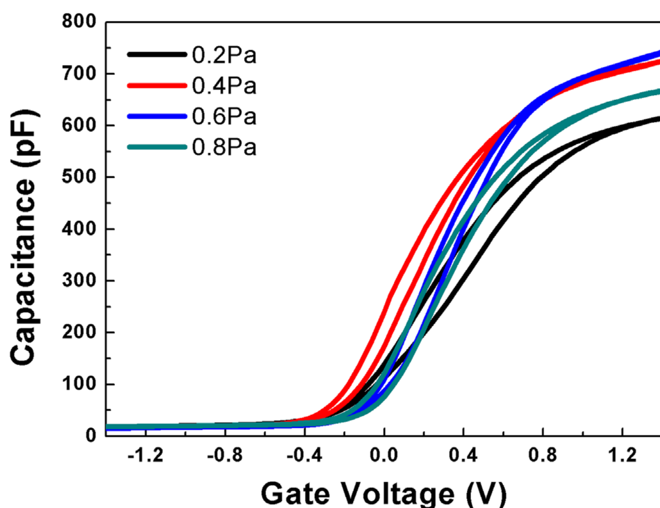

Fig. 11. Capacitance–voltage (*C*–*V*) characteristics curves for HfTiO gate dielectric MOS capacitors as a function of working pressure.

following expression: $N_{bt} = -(C_{\max}\,\Delta V_{fb})/qA$ [28]. The synchronous change of the border trapped oxide charge density and the hysteresis have been detected in Table 2. The ΔV_{fb} and the N_{bt} values of the sample deposited at 0.2 Pa are biggest, which is unfavorable for the high-k thin film. Based on above electrical analysis, the HfTiO thin film deposited at 0.6 Pa and 0.8 Pa have a good interface quality, which may bring about the preferable electrical properties.

As shown in Fig. 12, the asymmetry graph which manifest as the leakage current density *J* under negative bias voltage (gate injection) is higher than that under positive bias voltage (substrate injection) at the same absolute voltage value have been observed in *J*–*V* curves, which may be ascribed to the different carrier under the different injection mode [29] and different materials properties and conduction mechanism in the Al/HfTiO and HfTiO/Si interface [30,31]. As compared to others, the samples deposited at 0.2 and 0.4 Pa exhibits the high leakage current density when the same voltage value is applied to gate, which is likely due to the fact that the high oxide charge and trap charge reported in former electrical results induce the lowed conduction band offset [25]. The moderate packing density and lower oxide charge and trap charge density result in the lowest leakage current density of 1.39×10^{-5} A/cm^2 at bias voltage of 2 V for HfTiO thin film deposited at 0.6 Pa. The interface control is a decisive factor for the electrical property of MOSFET device.

Based on the above analysis, the HfTiO thin film with the working pressure of 0.6 Pa presents the best interface between HfTiO and Si substrate for the highest permittivity and lowest oxide and trap charge density.

The current conduction mechanism (CCM) of Al/HfTiO/Si device deposited at 0.6 Pa were investigated under gate injection to further analyze the charge transportation mechanism. There are many current conduction mechanisms existing at different electric filed regions, including the Pool–Frenkel (P–F), Schottky emission,

Table 2
Parameters of the MOS capacitors extracted from C–V curves.

Working pressure (Pa)	C_{ox} (pF)	E_{ot} (nm)	K	C_{fb} (pF)	V_{fb} (V)	N_{total} (cm^{-2})	ΔV_{fb} (V)	N_{bt} (cm^{-2})
0.2	615	3.97	31.20	93	−0.06	6.50×10^{11}	0.16	8.7×10^{11}
0.4	725	3.96	38.63	75	−0.16	1.48×10^{12}	0.07	4.7×10^{11}
0.6	740	3.30	39.92	63	−0.07	9.16×10^{11}	0.02	1.3×10^{11}
0.8	665	3.67	29.72	106	0.05	5.88×10^{10}	0.08	4.7×10^{11}

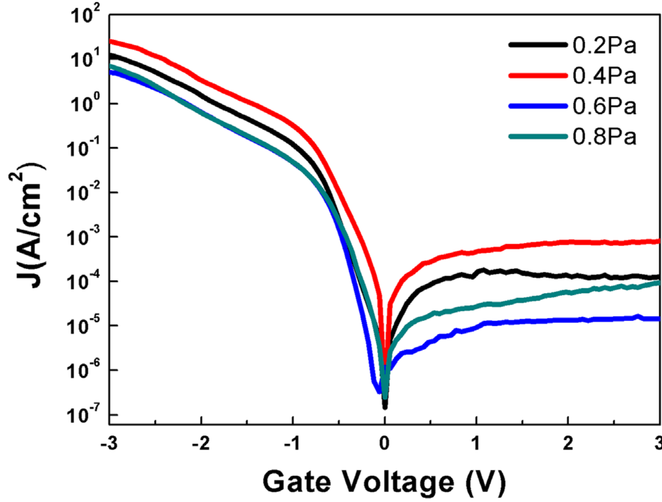

Fig. 12. Leakage current density–gate voltage (J–V) characteristics curves for HfTiO gate dielectric MOS capacitors as a function of working pressure.

Fowler–Nordheim (F–N), direct tunneling emission, ohmic transportation, and the space-charge-limited current. When the PF conduction mechanism works, the trapped electrons will transmit into the conduction band of insulator. The current density for PF is given by

$$J_{PF}=(q\mu N_C)E\,\exp\left[\frac{-q(\varphi_t-\sqrt{qE/\pi\varepsilon_0\varepsilon_{ox}})}{K_BT}\right] \quad (11)$$

In which J_{PF} is the current density, q is the electronic charge, μ is the electronic mobility in HfTiO thin film, N_C is the density of states in the conduction band, E is the applied electric filed, φ_t is the trap energy level below the conduction band edge of the dielectric, ε_{ox} is the oxide dielectric constant, respectively. Fig. 13(a) shows the plot of $\ln(J/E)$ versus $E^{1/2}$ at low electric field ($0.68< E<1.37$ MV/cm), which yields a straight line. The ε_{ox} obtained from the expression: Slope $=1/K_BT\sqrt{q^3/\pi\epsilon_{ox}}$ is about 3.5, which is much smaller than the reported values in literature [29,32], indicating the CCM of the HfTiO film at low electric field may do not meet the P–F emission. As the applied electric field further increases, the CCM of the HfTiO film convert into Schottky emission described as [33]

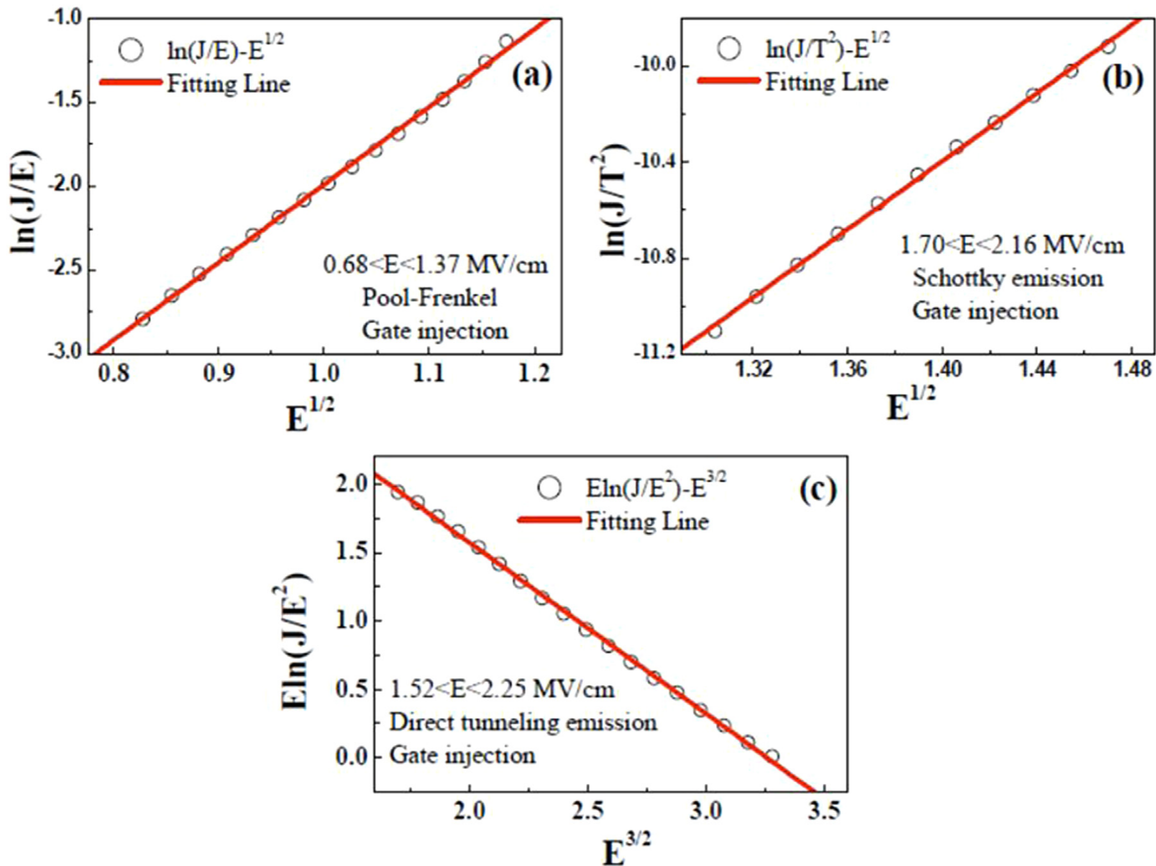

Fig. 13. Conduction mechanism fitting of 0.6 Pa deposited HfTiO thin film under gate injection. (a) The curve of $\ln(J/E)$ vs $E^{1/2}$ in low electric field; (b) the curve of $\ln(J/T^2)$ vs $E^{1/2}$ in high electric field; (c) the curve of $E\ln(J/E^2)$ vs $E^{3/2}$ in high electric field.

$$J_{SE} = A^{*}T^{2}\exp\left[\frac{-q(\phi_B - \sqrt{qE/4\pi\varepsilon_r\varepsilon_0})}{KT}\right] \quad (12)$$

In which A^{*} is the effective Richardson constant, T is the absolute temperature, ϕ_B is the Schottky barrier height, ε_r and ε_0 are the dynamic dielectric constant and the vacuum dielectric constant, respectively. Fig. 13(b) presents the plot of $\ln(J/T^2)$ versus $E^{1/2}$ for the HfTiO film at high electric field ($1.70 < E < 2.16$ MV/cm) and the linear behavior has been found, suggesting that the device exists a field-assisted thermionic emission mechanism. The n and ε_r can be calculated from the expression as following:

$$\text{slope} = \sqrt{\frac{q^3}{4\pi\epsilon_r\epsilon_0}} \quad (13)$$

$$\varepsilon_r = n^2 \quad (14)$$

The calculated n with the value of 2.06 is consistent with other report [28] and the result further shows that the Al/HfTiO/Si devices are dominated by the Schottky emission at high electric field. Besides, the linear fitting graphs of $E\ln(J/E^2)$ versus $E^{3/2}$ in the high electric field of $E > 1.52$ MV/cm are given in Fig. 13(c), indicating the direct tunneling emission also as a predominant conduction mechanism in high electric field.

4. Conclusion

To obtain the optimal working gas pressure, the effect of different working pressure on micro-structure, optical and electrical properties of HfTiO thin films fabricated by sputtering method with HfTi metal target and O_2 has been investigated in detail. It was found that all thin films remain amorphous despite of the working gas pressure, which meet the requirement of the evolution of MOS device. However, the working gas pressure has apparent impact on the optical and electrical properties. In the range of 0.2–0.4 Pa, the deposition rate, refraction index, and the extinction coefficient increases while the band gap decreases with the increase of the working gas pressure. Meanwhile, the increase in dielectric constant, flat band voltage, and total charge density have been detected with increased Ar gas pressure. When the thin films were deposited from 0.4 Pa through 0.6–0.8 Pa, the deposition rate, refraction index, and the extinction coefficient decreases and is lower than that deposited at 0.2 Pa while the band gap increases and higher than that deposited at 0.2 Pa. For the thin film deposited at 0.6 Pa, two types of leakage current conduction mechanisms, the Schottky emission and the direct tunneling emission are the dominant current conduction mechanism at higher electric fields. It is noted that the HfTiO film deposited at 0.6 Pa have the lowest total charge density and border trap charge density, as well as the highest permittivity. Therefore, the HfTiO thin film deposited at 0.6 Pa with the moderate band gap of 3.70 eV show potential application for future MOS devices.

Acknowledgments

The authors acknowledge the support from National Key Project of Fundamental Research (2013CB632705), National Natural Science Foundation of China (51572002, and 11474284), Anhui Provincial Natural Science Foundation (1608085MA06), and Outstanding Young Scientific Foundation of Anhui University (KJJQ1103) and “211 project” of Anhui University.

References

[1] C. Ye, Y. Wang, J. Zhang, J.Q. Zhang, H. Wang, Y. Jiang, Evidence of interface conversion and electrical characteristics improvement of ultrathin HfTiO films upon rapid thermal annealing, Appl. Phys. Lett. 99 (2011) 182904-1–182904-3.

[2] G. He, J.W. Liu, H.S. Chen, Y.M. Liu, Z.Q. Sun, X.S. Chen, M. L, L. Zhang, Interface control and modification of band alignment and electrical properties of HfTiO/GaAs gate stacks by nitrogen incorporation, J. Mater. Chem. C 2 (2014) 5299–5308.

[3] J.Q. Zhang, Z.X. Li, H. Zhou, C. Ye, H. Wang, Electrical, optical and micro-structural properties of ultra-thin HfTiON films, Appl. Surf. Sci. 294 (2014) 58–65.

[4] J.W. Liu, M.Y. Liao, M. Imura, A. Tanaka, H. Iwai, Y. Koide, Low on-resistance diamond field effect transistor with high-k ZrO_2 as dielectric, Sci. Rep. 4 (2014) 6395-1–6395-5.

[5] J.W. Liu, M.Y. Liao, M. Imura, E. Watanabe, H. Oosato, Y. Koide, Diamond field effect transistors with a high-dielectric constant Ta_2O_5 as gate material, J. Phys. D: Appl. Phys. 47 (2014) 245102-1–245102-5.

[6] G. He, L.Q. Zhu, M. Liu, Q. Fang, L.D. Zhang, Optical and electrical properties of plasma-oxidation derived HfO_2 gate dielectric films, Appl. Surf. Sci. 253 (2007) 3413–3418.

[7] J.W. Liu, M.Y. Liao, M. Imura, H. Oosato, E. Watanabe, Y. Koide, Electrical characteristics of hydrogen-terminated diamond metal–oxide–semiconductor with atomic layer deposited HfO_2 as gate dielectric, Appl. Phys. Lett. 102 (2013) 112910-1–112910-4.

[8] J.W. Zhang, G. He, L. Zhou, H.S. Chen, X.S. Chen, X.F. Chen, B. Deng, J.G. Lv, Z. Q. Sun, Microstructure optimization and optical and interfacial properties modulation of sputtering-derived HfO_2 thin films by TiO_2 incorporation, J. Alloy. Comp. 611 (2014) 253–259.

[9] F. Chen, X. Bin, C. Hella, X. Shi, W.L. Gladfelter, S.A. Campbell, A study of mixtures of HfO_2 and TiO_2 as high-k gate dielectrics, Microelectron. Eng. 72 (2004) 263–266.

[10] G.D. Wilk, R.M. Wallace, J.M. Anthony, High-k gate dielectrics: current status and materials properties considerations, J. Appl. Phys. 89 (2001) 5243–5275.

[11] P. Jin, G. He, M. Liu, D.Q. Xiao, J. Gao, X.F. Chen, R. Ma, J.W. Zhang, M. Zhang, Z. Q. Sun, Y.M. Liu, Deposition-power-modulated optical and electrical properties of sputtering-derived $HfTiO_x$ gate dielectrics, J. Alloy. Compd. 649 (2015) 128–134.

[12] C. Ye, C. Zhan, J.Q. Zhang, H. Wang, T.F. Deng, S.R. Tang, Influence of rapid thermal annealing temperature on structure and electrical properties of high permittivity HfTiO thin film used in MOSFET, Microelectron. Reliab. 54 (2014) 388–392.

[13] J.W. Liu, M.Y. Liao, M. Imura, Y. Koide, Normally-off HfO_2-gated diamond field effect transistors, Appl. Phys. Lett. 103 (2013) 092905 – 1–092905-4.

[14] M. Liu, L.D. Zhang, G. He, X.J. Wang, M. Fang, Effect of Ti incorporation on the interfacial and optical properties of HfTiO thin films, J. Appl. Phys. 108 (2010) 024102-1–024102-4.

[15] D. Patel, M. Patel, Leakage current reduction techniques for CMOS circuits, Int. J. Eng. Sci. 3 (2014) 1363–1366.

[16] J.W. Zhang, G. He, J. Gao, X.S. Chen, X.F. Chen, B. Deng, Y.M. Liu, M. Zhang, J. G. Lv, Z.Q. Sun, Annealing temperature dependent microstructure and optical properties of $Hf_xTi_{1-x}O_2$ thin films, Sci. Adv. Mater. 6 (2014) 1–7.

[17] C.S. Prajapati, P.P. Sahay, Influence of In doping on the structural, optical and acetone sensing properties of ZnO nanoparticulate thin films, Mater. Sci. Semicond. Process. 16 (2013) 200–210.

[18] S. Kosea, E. Ketenci, V. Bilgin, F. Atay, I. Akyuz a, Some physical properties of In doped copper oxide films produced by ultrasonic spray pyrolysis, Curr. Appl. Phys. 12 (2012) 890–895.

[19] Y.J. Cho, W.J. Lee, C.Y. Kim, M.H. Cho, H. Kim, H.J. Lee, D.W. Moon, H.J. Kang, Band gap change and interfacial reaction in Hf-silicate film grown on Ge(001), J. Chem. Phys. 129 (2008) 164117 – 1–164117-4.

[20] M.C. Cisneros-Morales, C.R. Aita, The effect of nanocrystallite size in monoclinic HfO_2 films on lattice expansion and near-edge optical absorption, Appl. Phys. Lett. 96 (2010) 191904-1–191904-3.

[21] Z.W. Ma, Y.R. Su, Y.Z. Xie, H.T. Zhao, L.X. Liu, J. Li, E.Q. Xie, Influence of gas pressure on the structural and optical of sputtered properties of Hafnium oxide thin film, Mater. Rev. 26 (2012) 16–22.

[22] B.C. Yang, W.S. Wang, Physics and Technology of Thin Films, Electronic science & Technology University Press, Chengdou, 1994, p. 81.

[23] L. Wang, O.M. Yu, L.X. Hang, B.P. Zhao, Z.H. Wang, Influence of the working gas pressure on the deposition rate in magnetron sputtering for thin coating, Vacuum 41 (2004) 10–12.

[24] W.T. Liu, Z.T. Liu, F. Yan, T.T. Tan, H. Tian, Influence of O_2/Ar flow ratio on the structure and optical properties of sputtered hafnium dioxide thin films, Surf. Coat. Technol. 205 (2010) 2120–2125.

[25] J. Gao, G. He, B. Deng, D.X. Xiao, M. Liu, P. Jin, C.Y. Zheng, Z.Q. Sun, Microstructure, wettability, optical and electrical properties of HfO_2 thin films: effect of oxygen partial pressure, J. Alloy. Compd. 622 (2016) 339–347.

[26] J.B. Fan, H.X. Liu, Q.W. Kuang, B. Gao, F. Ma, Y. Hao, Physical properties and electrical characteristics of H_2O-based and O_3-based HfO_2 films deposited by ALD, Microelectron. Reliab. 52 (2012) 1043–1049.

[27] P.T. Lai, S. Chakraborty, C.L. Chan, Y.C. Cheng, Effects of nitridation and annealing on interface properties of thermally oxidized SiO_2/SiC metal–oxide–semiconductor system, Appl. Phys. Lett. 76 (2000) 3744–3746.

[28] H.J. Quah, W.F. Lim, K.Y. Cheong, Z. Hassan, Z. Lockman, Comparison of metal-organic decomposed (MOD) cerium oxide (CeO_2) gate deposited on GaN and SiC substrates, J. Cryst. Growth 326 (2011) 2–8.

[29] J.W. Zhang, G. He, M. Liu, H.S. Chen, Y.M. Liu, Z.Q. Sun, X.S. Chen, Composition dependent interfacial thermal stability, band alignmentand electrical properties of $Hf_{1-x}Ti_xO_2$/Si gate stacks, Appl. Surf. Sci. 346 (2015) 489–496.

[30] H. Wang, Y. Wang, J. Zhang, C. Ye, H.B. Wang, J. Feng, B.Y. Wang, Q. Li, Y. Jiang, Interface control and leakage current conduction mechanism in HfO_2 film prepared by pulsed laser deposition, Appl. Phys. Lett. 93 (2008) 202904-1–202904-3.

[31] A.P. Huang, P.K. Chu, Improvement of interfacial and dielectric properties of sputtered Ta_2O_5 thin films by substrate biasing and the underlying mechanism, Appl. Phys. Lett. 97 (2005) 114106 – 1–114106-5.

[32] J.W. Zhang, G. He, H.S. Chen, J. Gao, X.F. Chen, P. Jin, D.Q. Xiao, R. Ma, M. Liu, Z. Q. Sun, Modulation of charge trapping and current-conduction mechanism of TiO_2-doped HfO_2 gate dielectrics based MOS capacitors by annealing temperature, J. Alloy. Compd. 647 (2015) 1054–1060.

[33] S.J. Ding, D.W. Zhang, L.K. Wang, Atomic-layer-deposited Al_2O_3-HfO_2 laminated and sandwiched dielectrics for metal–insulator–metal capacitors, J. Phys. D: Appl. Phys. 40 (2007) 1072–1076.